Hexadentate N_3O_3 Amine Phenol Ligands for Group 13 Metal Ions: Evidence for Intrastrand and Interstrand Hydrogen-Bonds in Polydentate Tripodal Amine Phenols

Shuang Liu,[1] Ernest Wong, Steven J. Rettig, and Chris Orvig*

Department of Chemistry, University of British Columbia, 2036 Main Mall, Vancouver, British Columbia V6T 1Z1, Canada

Received April 21, 1993®

Several N_3O_3 amine phenols (H_3**L1** = 1,2,3-tris((2-hydroxybenzyl)amino)propane; H_3**L2** = 1,2,3-tris((5-chloro-2-hydroxybenzyl)amino)propane; H_3**L3** = 1,2,3-tris((2-hydroxy-5-methoxybenzyl)amino)propane; H_3**L4** = 1,2,3-tris((3,5-dichloro-2-hydroxybenzyl)amino)propane) were prepared and characterized by various spectroscopic methods (IR, FAB-MS, NMR). The N_3O_3 amine phenols are KBH_4 reduction products of the corresponding Schiff bases derived from the condensation reactions of tap (tap = 1,2,3-triaminopropane) with 3 equiv of either salicylaldehyde or ring-substituted salicylaldehydes. Neutral binary metal complexes, [M(L)] (M = Al, L = **L2**, **L4**; M = Ga, In, L = **L1**–**L4**), were obtained from the reactions of Al^{3+}, Ga^{3+}, or In^{3+} with N_3O_3 amine phenols in the presence of 3 equiv of a base (acetate or hydroxide). The molecular structure of [Ga(**L3**)]·$2CH_3OH$ was determined by X-ray methods. Crystals of [Ga(**L3**)]·$2CH_3OH$ are monoclinic, of space group $P2_1/n$, with a = 13.115(3) Å, b = 15.674(2) Å, c = 14.439(2) Å, β = 100.62(1)°, and Z = 4. The structure of [Ga(**L3**)]·$2CH_3OH$ was solved by the Patterson method and was refined by full-matrix least-squares procedures to R = 0.028 for 4529 reflections with $I \geq 3\sigma(I)$. In [Ga(**L3**)]·$2CH_3OH$, the Ga atom is coordinated by six (N_3O_3) donor atoms in a slightly distorted octahedral coordination geometry. The cavity of the tap-based N_3O_3 amine phenol ligand matches well the size of Ga^{3+}. Variable-temperature ^1H NMR spectral data revealed rigid solution structures for all the aluminum, gallium, and indium complexes, with no evidence for fluxional behavior; the complexes remained very rigid at solution temperatures higher than 120 °C. Reaction of H_3**L1** with acetone produces a new amine phenol H_3L' containing a 2,2-dimethylimidazolidine ring. The molecular structure of H_3L' was determined by X-ray methods. Crystals of H_3L' are triclinic, $P\bar{1}$, with a = 10.8209(8) Å, b = 12.436(1) Å, c = 9.1556(8) Å, α = 92.561(9)°, β = 101.028(6)°, γ = 84.506(8)°, and Z = 2. The structure of H_3L' was solved by direct methods and was refined by full-matrix least-squares procedures to R = 0.036 for 2825 reflections with $I \geq 3\sigma(I)$. The H_3L' structural data revealed strong intrastrand (O–H- - -N) and very weak interstrand (N–H- - -N) H-bonds, which contribute, at least in part, to the highly preorganized ligand framework of polydentate tripodal amine phenols.

Introduction

There is currently considerable interest in the design of polydentate chelating ligand systems, which form stable complexes with group 13 metal ions, either for the treatment of Al overload or for the development of Ga and In radiopharmaceuticals.[2,3] We are interested in tripodal polydentate amine phenol ligands because of the high affinity of phenolate O and neutral N donors for trivalent metal ions[4] and because of the three-dimensional cavities imposed by the preorganized framework. Recently, we reported[5-8] two tripodal amine phenol ligand systems (Chart I): Tren-based (tren = tris(2-aminoethyl)amine) N_4O_3 amine phenols **I**,[5,6,8] in which three chelating arms were bridged by a tertiary nitrogen atom, and tame-based (tame = 1,1,1-tris(aminomethyl)ethane) N_3O_3 amine phenols **II**,[7] wherein the three chelating arms were bridged by a tertiary carbon atom. We found that the coordination modalities of the tren-based N_4O_3 amine phenol ligands depended on the size and donor atom selectivity of metal ions, while the tame-based N_3O_3 analogus were highly flexible and better tailored to form six-coordinate neutral complexes with Al^{3+}, Ga^{3+}, and In^{3+}.[5-8] Since the three chelating arms in the tame-based N_3O_3 amine phenols were bridged by a tertiary carbon atom, they could not undergo an "umbrella" type inversion. From this point of view, the C-bridged framework offered a higher degree of preorganization than did the N-bridged case.

Chart I

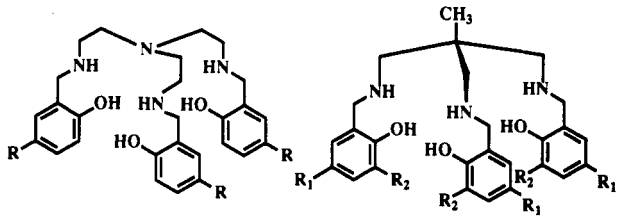

H_3**IIa**, R = H
H_3**IIb**, R = Cl
H_3**IIc**, R = Br

H_3**IIa**: R_1=R_2=H H_3**IIb**: R_1=Cl, R_2=H
H_3**IIc**: R_1=Br, R_2=H H_3**IId**: R_1=R_2=Cl

I II

1,2,3-Triaminopropane (tap) is the smallest aliphatic triamine. Due to the paucity of highly efficient synthetic methods for tap, scant attention has been paid to its coordination chemistry since the 1920s.[9] Recently, Tasker and co-workers reported a highly efficient synthesis of tap via the reduction of the corresponding triazide by hydrazine hydrate/palladium on carbon, lithium aluminum hydride, or sodium borohydride.[10] However, no studies

* To whom correspondence should be addressed. Phone: 604-822-4449. FAX: 604-822-2847.

® Abstract published in *Advance ACS Abstracts*, September 1, 1993.

(1) Natural Sciences and Engineering Research Council Postdoctoral Fellow, 1991–1993.
(2) Clevette, D. J.; Orvig, C. *Polyhedron* **1990**, *9*, 151.
(3) Zhang, Z.; Lyster, D. M.; Webb, G. A.; Orvig, C. *Nucl. Med. Biol.* **1992**, *19*, 327.
(4) Duma, T. W.; Marsicano, F.; Hancock, R. D. *J. Coord. Chem.* **1991**, *23*, 221.
(5) Liu, S.; Gelmini, L.; Rettig, S. J.; Orvig, C. *J. Am. Chem. Soc.* **1992**, *114*, 6081.
(6) Liu, S.; Rettig, S. J.; Orvig, C. *Inorg. Chem.* **1992**, *31*, 5400.
(7) Liu, S.; Wong, E.; Karunaratne, V.; Rettig, S. J.; Orvig, C. *Inorg. Chem.* **1993**, *32*, 1756.
(8) Liu, S.; Yang, L.-W.; Rettig, S. J.; Orvig, C. *Inorg. Chem.* **1993**, *32*, 2773.
(9) Black, D. St. C. *Coord. Chem. Rev.* **1972**, *9*, 219 and references therein.
(10) Henrick, K.; McPartlin, M.; Munjoma, S.; Owston, P. G.; Peters, R.; Sangokoya, S. A.; Tasker, P. A. *J. Chem. Soc., Dalton Trans.* **1982**, 225.

0020-1669/93/1332-4268$04.00/0

Chart II

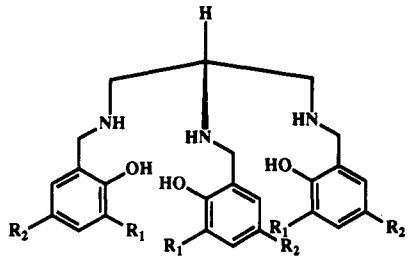

H_3L1: $R_1 = R_2 = H$
H_3L2: $R_1 = H$, $R_2 = Cl$
H_3L3: $R_1 = H$, $R_2 = OCH_3$
H_3L4: $R_1 = R_2 = Cl$

have been reported on tap-based Schiff bases and their corresponding amine phenols.

We have chosen to explore the coordination chemistry of the amine phenols derived from tap (Chart II) to delineate the influence of changes in ligand framework on the fit between the size of cavity of an amine phenol ligand and the size of a coordinated metal ion. In our previous contributions,[5-7] we found that the cavity of the tren-based N_4O_3 amine phenol ligand (I) matched best the size of In^{3+} while that of a tame-based N_3O_3 analog (II) fit perfectly the size of Al^{3+}. One of the three chelating arms of the tap-based N_3O_3 amine phenol ligand is shortened by one methylene linkage relative to the corresponding tame-based analogs. This should influence the binding of the ligand to the metal ion and the symmetry of the resulting metal complex. Furthering our investigation into the coordination chemistry of the group 13 metals with polydentate amine phenol ligands, we now present the synthesis and structural and spectroscopic properties of aluminum, gallium, and indium complexes of several new tap-based N_3O_3 amine phenols (H_3L1–H_3L4).

Experimental Section

Materials. Potassium borohydride, lithium aluminum hydride, sodium azide, hydrated metal salts, salicylaldehyde, 5-chlorosalicylaldehyde, 3,5-dichlorosalicylaldehyde, and 5-methoxysalicylaldehyde were obtained from Aldrich or Alfa and were used without further purification. 1,2,3-Tris(azidomethyl)propane was prepared according to the literature method.[10]

Instrumentation. NMR spectra (200, 300, 400, and 500 MHz) were recorded on Bruker AC-200E (^1H, ^{13}C, and APT ^{13}C NMR), Varian XL 300 (VT NMR), Varian XL 400 (^1H–^1H COSY NMR), and Varian XL 500 (^1H–^{13}C heteronuclear correlation) spectrometers, respectively. Mass spectra were obtained with either a Kratos MS 50 (electron-impact ionization, EI) or a Kratos Concept II H32 Q (fast-atom-bombardment ionization, FAB) instrument. Infrared spectra were recorded as KBr disks in the range 4000–400 cm^{-1} on a Perkin-Elmer PE 783 spectrophotometer and were referenced to polystyrene. Melting points were measured on a Mel-Temp apparatus and are uncorrected. Analyses for C, H, and N were performed by Mr. Peter Borda in this department.

Ligand Syntheses. *Caution! The handling of polyazides in large quantities may be hazardous. Perchlorate salts of metal complexes are potentially explosive and should be handled with care and only in small amounts.*

1,2,3-Triaminopropane (tap). Tap was prepared according to the reported method[10] with some modifications. To a 0 °C solution of 1,2,3-triazidopropane (29 g, 0.18 mol) in dry THF (500 mL) was added slowly $LiAlH_4$ (25 g, 0.62 mmol) over a period of 30 min, and then the mixture was heated to reflux for 24 h. The mixture was cooled to 0 °C, and 8 M NaOH (50 mL) was added slowly to quench the excess $LiAlH_4$. To the resulting white slurry was added diethyl ether (500 mL), and the mixture was stirred for 30 min. The white precipitate was filtered off and washed with diethyl ether (2 × 200 mL). The combined filtrates were dried over anhydrous $MgSO_4$; upon removal of solvent on a rotary evaporator, a pale-yellow oil was obtained. Yield: 8.6 g (70%). The IR and ^1H NMR spectra of the crude product were identical with those reported for tap.[10] This crude product was used without further purification.

1,2,3-Tris(salicylideneamino)propane (H_3saltap). To a solution of salicylaldehyde (3.6 g, 30 mmol) in absolute ethanol (5 mL) was added tap (0.89 g, 10 mmol) in diethyl ether (5 mL). The mixture was left standing at room temperature until bright yellow microcrystals deposited. These were separated from the mixture, washed with diethyl ether, and dried in air. Yield: 3.5 g (77%). Mp: 139–140 °C. Anal. Calcd (found) for $C_{24}H_{23}N_3O_3$: C, 71.80 (71.84); H, 5.77 (5.77); N, 10.47 (10.47). Mass spectrum (EI): m/z = 401 (M^+, $[C_{24}H_{23}N_3O_3]^+$). IR (cm^{-1}, KBr disk): 3450 (br, ν_{O-H}); 3000–2800 (m, ν_{C-H}); 1630, 1610, 1580, 1495 (vs, $\nu_{C=N}$, $\nu_{C=C}$).

1,2,3-Tris((5-chlorosalicylidene)amino)propane (H_3Cl-saltap). To a hot solution of 5-chlorosalicylaldehyde (4.7 g, 30 mmol) in absolute ethanol (50 mL) was added tap (0.89 g, 10 mmol) in 5 mL of the same solvent. The resulting yellow solution was refluxed for about 30 min and then cooled to room temperature. Slow evaporation of the solvent afforded an orange-yellow solid, which was collected by filtration, washed with absolute ethanol and diethyl ether, and dried in air. Yield: 4.5 g (80%). Mp: 123–125 °C. Anal. Calcd (found) for $C_{24}H_{20}Cl_3N_3O_3$: C, 57.10 (57.22); H, 3.99 (4.07); N, 8.32 (8.19). Mass spectrum (EI): m/z = 503 (M^+, $[C_{24}H_{20}Cl_3N_3O_3]^+$). IR ($cm^{-1}$, KBr disk): 3450 (br, ν_{O-H}); 1635, 1575, 1478 (vs, $\nu_{C=N}$, $\nu_{C=C}$).

1,2,3-Tris((5-methoxysalicylidene)amino)propane (H_3psaltap). A procedure similar to that for H_3saltap was followed using 5-methoxysalicylaldehyde (6.03 g, 30 mmol) and tap (0.89 g, 10 mmol). Yield: 4.5 g (80%). Mp: 150–151 °C. Anal. Calcd (found) for $C_{27}H_{29}N_3O_6$: C, 65.98 (66.08); H, 5.95 (6.01); N, 8.55 (8.53). Mass spectrum (EI): m/z = 491 (M^+, $[C_{27}H_{29}N_3O_6]^+$). IR (cm^{-1}, KBr disk): 3450 (w, ν_{O-H}); 3000–2800 (m, ν_{C-H}); 1635, 1570, 1505, 1455, 1440 (vs, $\nu_{C=N}$, $\nu_{C=C}$).

1,2,3-Tris((3,5-dichlorosalicylidene)amino)propane (H_3Cl_2saltap). A procedure similar to that above was employed using 3,5-dichlorosalicylaldehyde (6.03 g, 30 mmol) and tap (0.89 g, 10 mmol). Yield: 4.5 g (80%). Mp: 143–144 °C. Anal. Calcd (found) for $C_{24}H_{17}Cl_6N_3O_3$: C, 47.40 (47.23); H, 2.82 (3.00); N, 6.91 (6.88). Mass spectrum (EI): m/z = 607 (M^+, $[C_{24}H_{17}Cl_6N_3O_3]^+$). IR ($cm^{-1}$, KBr disk): 3450 (w, ν_{O-H}); 3000–2800 (m, ν_{C-H}); 1630, 1570, 1515, 1475 (vs, $\nu_{C=N}$, $\nu_{C=C}$).

1,2,3-Tris((2-hydroxybenzyl)amino)propane (H_3L1). To a solution of H_3saltap (2.15 g, 5 mmol) in methanol (100 mL) was added KBH_4 (1.08 g, 20 mmol) in small portions at room temperature over 30 min. After the addition was complete, the reaction mixture was stirred at room temperature for an additional 30 min. The solvent was removed under reduced pressure. To the residue was added NH_4OAc (3 g) in water (50 mL), and the mixture was extracted with chloroform (3 × 100 mL). The organic phases were combined, washed with water, and dried over anhydrous $MgSO_4$. The solution was filtered and chloroform was removed on a rotary evaporator to afford a pale-yellow solid. The solid was dried under vacuum overnight. Yield: 1.9 g (87%). Mp: 60–63 °C. Anal. Calcd (found) for $C_{24}H_{29}N_3O_3 \cdot 0.5H_2O$: C, 69.21 (68.88); H, 7.26 (7.16); N, 10.09 (9.72). Mass spectrum (FAB): m/z = 408 ([M + 1]$^+$, $[C_{24}H_{30}N_3O_3]^+$). IR (cm^{-1} KBr disk): 3500–2000 (m, ν_{N-H}, ν_{O-H}); 1615, 1605, 1585 (s, δ_{N-H}); 1500–1400 (vs, $\nu_{C=C}$).

1,2,3-Tris((2-hydroxy-5-chlorobenzyl)amino)propane (H_3L2). A procedure similar to that for H_3L1 was followed using H_3Cl-saltap (2.35 g, 5.0 mmol) and KBH_4 (1.08 g, 20 mmol). Yield: 2.50 g (73%). Mp: 72–75 °C. Anal. Calcd (found) for $C_{24}H_{26}Cl_3N_3O_3 \cdot 0.5H_2O$: C, 55.45 (55.60); H, 5.23 (5.15); N, 8.08 (8.00). Mass spectrum (FAB): m/z = 512, 510 ([M + 1]$^+$, $[C_{24}H_{27}Cl_3N_3O_3]^+$). IR ($cm^{-1}$, KBr disk): 3340–3290 (m, ν_{N-H}, ν_{O-H}); 1610, 1583 (s, δ_{N-H}); 1480 (vs, $\nu_{C=C}$).

1,2,3-Tris((2-hydroxy-5-methoxybenzyl)amino)propane (H_3L3). This was prepared in a manner similar to that for H_3L1 employing H_3psaltap (2.5 g, 5.0 mmol) and KBH_4 (1.08 g, 20 mmol). Yield: 2.50 g (73%). Mp: 32–35 °C. Anal. Calcd (found) for $C_{27}H_{35}N_3O_6 \cdot 0.75H_2O$: C, 63.45 (63.34); H, 7.20 (7.00); N, 8.22 (8.07). Mass spectrum (FAB): m/z = 498 ([M + 1]$^+$, $[C_{27}H_{35}N_3O_6]^+$). IR (cm^{-1}, KBr disk): 3600–2500 (br, ν_{O-H}, ν_{N-H}); 3000–2800 (m, ν_{C-H}); 1615, 1590 (m, δ_{N-H}); 1490–1420 (vs, $\nu_{C=C}$).

1,2,3-Tris((3,5-dichloro-2-hydroxybenzyl)amino)propane (H_3L4). To a hot solution of H_3Cl_2saltap (2.5 g, 5.0 mmol) in methanol (150 mL) was added KBH_4 (1.25 g, 20 mmol) in small portions at room temperature over 45 min. After the addition was complete, the reaction mixture was stirred at room temperature for an additional 30 min. The solvent was removed under reduced pressure. To the residue was added NH_4OAc (5 g) in water (50 mL), and a white precipitate formed. The precipitate was isolated by filtration, washed with water, and dried under vacuum overnight. Yield: 2.50 g (73%). Mp: 165–170 °C. Anal. Calcd (found) for $C_{24}H_{23}Cl_6N_3O_3 \cdot 1.5H_2O$: C, 44.96 (44.68); H, 4.09 (3.78); N, 6.55 (5.99). Mass spectrum (FAB): m/z = 614 ([M + 1]$^+$, $[C_{24}H_{24}$-

Table I. Analytical Data (Calcd (Found)) for Al, Ga, and In Complexes of Tap-Based N_3O_3 Amine Phenols

compound	C	H	N
[Al(**L2**)]·4H_2O·0.5$CHCl_3$	44.15 (44.27)	4.76 (4.43)	6.30 (6.07)
[Al(**L4**)]·2CH_3OH	44.47 (44.11)	4.02 (3.84)	5.98 (6.13)
[Ga(**L1**)]·3H_2O	54.57 (54.30)	6.11 (5.64)	7.95 (7.86)
[Ga(**L2**)]·H_2O·CH_3OH	47.84 (47.96)	4.66 (4.51)	6.70 (6.74)
[Ga(**L3**)]·2CH_3OH	55.43 (55.30)	6.42 (6.54)	6.69 (6.47)
[Ga(**L4**)]·2.5H_2O	39.71 (39.78)	3.47 (3.34)	5.79 (5.86)
[In(**L1**)·4.5H_2O	48.01 (48.04)	5.88 (5.79)	7.00 (7.05)
[In(**L2**)·4H_2O	41.49 (42.33)	4.50 (4.11)	6.05 (5.77)
[In(**L3**)]·2.5H_2O	49.55 (49.60)	5.70 (5.59)	6.42 (6.67)
[In(**L4**)]·CH_3OH	39.61 (39.37)	3.19 (3.28)	5.54 (5.20)

Table II. Infrared (cm^{-1}, KBr disk) and FAB Mass Spectral Data for Al, Ga, and In Complexes of Tap-Based N_3O_3 Amine Phenols

			m/z	
compound	ν_{O-H} and ν_{N-H}	δ_{N-H}	$[ML + 1]^+$	$[2ML + 1]^+$
[Al(**L2**)]·4H_2O·0.5$CHCl_3$	3700–2800 b, s; 3260 m	1595 s; 1570 w	534, 536	1069
[Al(**L4**)]·2CH_3OH	3700–3000 b, s; 3265 m	1585 m; 1550 w	638	1277
[Ga(**L1**)]·3.5H_2O	3650–3000 b, s; 3260 s	1595 s, 1570 m	474	949
[Ga(**L2**)]·H_2O·CH_3OH	3700–3000 b, s; 3265 s	1590 s; 1560 w	578	1155
[Ga(**L3**)]·2CH_3OH	3700–3000 b, s; 3265 s	1595 s; 1560 w	564	1129
[Ga(**L4**)]·2.5H_2O	3700–2800 b, s; 3275 s	1590 m; 1550 w	682	
[In(**L1**)]·4.5H_2O	3700–2800 b, s; 3260 s	1595 s; 1565 m	520	1039
[In(**L2**)]·4H_2O	3700–2200 b, s; 3275 s	1595 s; 1560 s	622	1245
[In(**L3**)·2.5H_2O	3700–3000 b, s; 3275 m	1585 s	610	1219
[In(**L4**)]·CH_3OH	3700–2500 b, s; 3250 s	1575 m; 1560 s	726	

$Cl_6N_3O_3]^+$). IR (cm^{-1}, KBr disk): 3600–2500 (br, ν_{O-H}, ν_{N-H}); 3000–2800 (m, ν_{C-H}); 1615, 1590 (s, δ_{N-H}); 1490–1420 (vs, $\nu_{C=C}$).

Reaction of Tap-Based Amine Phenol with Acetone (H_3L'). H_3L1 (0.41 g, 1.0 mmol) was dissolved in acetone (50 mL), and the solution was refluxed for 2 h. The solution was cooled to room temperature; slow evaporation afforded a white microcrystalline solid. The solid was collected by filtration, washed with a small amount of diethyl ether, and dried in air. Recrystallization from methanol produced crystals suitable for X-ray diffraction studies. Yield: 0.35 g (54%). Mp: 89–92 °C. Anal. Calcd (found) for $C_{27}H_{33}N_3O_3$·0.25H_2O: C, 71.73 (71.93); H, 7.47 (7.35); N, 9.29 (9.17). Mass spectrum (FAB): m/z = 448 ($[M + 1]^+$, $[C_{27}H_{34}N_3O_3]^+$). IR (cm^{-1}, KBr disk): 3600–2500 (br, ν_{O-H}, ν_{N-H}): 3000–2800 (m, ν_{C-H}); 1610, 1585 (s, δ_{N-H}); 1500–1400 (vs, $\nu_{C=C}$).

Metal Complex Syntheses. Since many of the syntheses were similar, detailed procedures are only given for representative examples. The yields ranged from 40% to 80%. All prepared complexes, with their analytical data, are listed in Table I. Infrared and FAB mass spectral data are given in Table II.

[Al(L2)]·4H_2O·0.5$CHCl_3$. To a solution of $Al(ClO_4)_3$·9H_2O (240 mg, 0.50 mmol) and H_3L2 (240 mg, 0.53 mmol) in methanol (30 mL) was added 2 M NaOH (1.5 mL). The mixture was filtered immediately, and the filtrate was left in the fumehood. Slow evaporation of solvents produced a crystalline solid. Recrystallization from 1:1 methanol/chloroform afforded the pure complex in a yield of 162 mg (45%).

[Ga(L3)]·2CH_3OH. Method 1. To a solution of $Ga(NO_3)_3$·9H_2O (209 mg, 0.5 mmol) in methanol (20 mL) was added H_3L3 (250 mg, 0.5 mmol) in the same solvent (10 mL). After the dropwise addition of 2 M NaOH (1 mL), the resulting mixture was filtered immediately. Slow evaporation of the solvents afforded pink crystals, which were collected by filtration, washed with cold ethanol followed by diethyl ether, and dried in air. The yield was 200 mg (71%). Suitable crystals were selected for X-ray diffraction study.

Method 2. Solutions of $Ga(NO_3)_3$·9H_2O (209 mg, 0.50 mmol) in methanol (25 mL) and of H_3L3 (240 mg, 0.53 mmol) in the same solvent (10 mL) were mixed. After addition of NaOAc·3H_2O (280 mg, 2.0 mmol) in methanol (5 mL), the mixture was filtered immediately. The filtrate was left standing at the room temperature to evaporate solvents slowly until pink microcrystals formed. These were separated from the mixture, washed with ethanol and diethyl ether, and dried in air. The product was shown by IR and elemental analysis to be identical to that obtained by method 1.

Table III. Selected Crystallographic Data for H_3L' and [Ga(**L3**)]·2CH_3OH

formula	$C_{27}H_{33}N_3O_3$	$C_{29}H_{40}GaN_3O_8$
fw	447.58	628.37
crystal syst	triclinic	monoclinic
space group	$P\bar{1}$	$P2_1/n$
a, Å	10.8209(8)	13.115(3)
b, Å	12.436(1)	15.674(2)
c, Å	9.1556(8)	14.349(2)
α, deg	92.561(9)	
β, deg	101.028 (6)	100.62(1)
γ, deg	84.506(8)	
V, Å^3	1203.3(2)	2899.0(7)
Z	2	4
ρ_c, g/cm^3	1.235	1.439
T, °C	21	21
radiation (λ, Å)	Cu (1.541 78)	Cu (1.541 78)
μ(Cu Kα), cm^{-1}	6.10	17.25
transm factors	0.96–1.00	0.95–1.00
R	0.036	0.028
R_w	0.035	0.034

[In(L4)·CH_3OH. To a suspension of H_3L4 (800 mg, 1.0 mmol) in 50 mL of 1:2 methanol/chloroform was added $In(NO_3)_3$·3H_2O (355 mg, 1.0 mmol) and NaOAc·3H_2O (556 mg, 4.0 mmol). The resulting mixture was filtered, and solvents were slowly evaporated at room temperature to give a pale-yellow solid. Recrystallization in methanol afforded a microcrystalline solid, which was collected by filtration, washed with cold ethanol followed by diethyl ether, and dried in air. The yield was 400 mg (53%).

X-ray Crystallographic Analyses. Selected crystallographic data for H_3L' and [Ga(**L3**)]·2CH_3OH appear in Table III. The final unit-cell parameters were obtained by least-squares calculations on the setting angles for 25 reflections with 2θ = 60.7–82.1° for H_3L' and 91.1–108.3° for [Ga(**L3**)]·2CH_3OH. The intensities of three standard reflections, measured every 200 reflections throughout the data collections, showed only small random fluctuations for H_3L' and decayed uniformly by 3.0% for [Ga(**L3**)]·2CH_3OH. The data were processed[11] and corrected for Lorentz and polarization effects, decay (for [Ga(**L3**)]·2CH_3OH), and absorption (empirical; based on azimuthal scans for three reflections).

The structure of H_3L' was solved by direct methods, and that of [Ga(**L3**)]·2CH_3OH, by conventional heavy-atom methods, the coordinates of the Ga atom being determined from the Patterson function and those of the remaining non-hydrogen atoms from subsequent difference Fourier syntheses. The structure analysis of H_3L' was initiated in the centrosymmetric space group $P\bar{1}$ on the basis of E-statistics, this choice being confirmed by the subsequent successful solution and refinement of the structure. The asymmetric unit of [Ga(**L3**)]·2CH_3OH contains the [Ga(**L3**)] complex and two molecules of methanol, both of which are hydrogen-bonded to the gallium complex.

All non-hydrogen atoms of both structures were refined with anisotropic thermal parameters. The O–H hydrogen atoms of H_3L' and [Ga(**L3**)]·2CH_3OH and the N–H hydrogen atoms of H_3L' were refined with isotropic thermal parameters. The remaining hydrogen atoms of both compounds were fixed in calculated positions (staggered methyl groups, C–H = 0.98 Å, B(H) = 1.2B(bonded atom)). Secondary extinction corrections were applied both cases, the final values of the extinction coefficient being 4.16(8) × 10^{-6} and 9.8(1) × 10^{-7}, respectively for H_3L' and [Ga(**L3**)]·2CH_3OH. Neutral-atom scattering factors for all atoms and anomalous dispersion corrections for the non-hydrogen atoms were taken from the ref 12. Final atomic coordinates and equivalent isotropic thermal parameters, bond lengths for H_3L', bond angles for H_3L', bond lengths for [Ga(**L3**)]·2CH_3OH, and bond angles for [Ga(**L3**)]·2CH_3OH appear in Tables IV–VIII, respectively. Complete tables of crystallographic data, hydrogen atom parameters, anisotropic thermal parameters, intramolecular distances and angles involving hydrogen atoms, torsion angles, intermolecular contacts, and least-squares planes for each of the two structures are included as supplementary material.

(11) TEXSAN/TEXRAY structure analysis package, Molecular Structure Corp., 1985.
(12) *International Tables for X-Ray Crystallography*; Kynoch Press: Birmingham, U.K. (present distributor: Kluwer Academic Publishers, Dordrecht, The Netherlands), 1974; Vol. IV, pp 99–102, 149.

Table IV. Final Atomic Coordinates (Fractional) and B_{eq} Values (Å^2)[a]

atom	x	y	z	B_{eq}	atom	x	y	z	B_{eq}
				H_3L1' ($C_{27}H_{33}N_3O_3$)					
O(1)	0.6402(2)	0.2031(2)	0.2825(2)	5.8(1)	C(12)	0.4409(2)	0.3945(2)	0.8734(2)	4.1(1)
O(2)	0.4579(2)	0.5066(1)	0.6722(2)	5.60(9)	C(13)	0.3890(2)	0.4745(2)	0.7722(2)	4.3(1)
O(3)	0.3455(1)	0.1409(1)	0.2219(2)	4.75(8)	C(14)	0.2670(2)	0.5202(2)	0.7660(3)	5.3(1)
N(1)	0.7014(1)	0.1913(1)	0.5843(2)	3.52(7)	C(15)	0.1947(2)	0.4851(2)	0.8599(3)	6.0(1)
N(2)	0.5904(1)	0.2978(1)	0.7312(2)	3.54(7)	C(16)	0.2425(3)	0.4054(2)	0.9589(3)	5.8(1)
N(3)	0.4097(2)	0.2788(1)	0.4498(2)	3.92(8)	C(17)	0.3653(3)	0.3612(2)	0.9660(2)	5.0(1)
C(1)	0.7232(2)	0.2686(2)	0.7133(2)	3.7(1)	C(18)	0.7793(2)	0.3670(2)	0.6698(3)	5.0(1)
C(2)	0.5190(2)	0.2013(2)	0.6895(2)	3.7(1)	C(19)	0.8073(2)	0.2187(2)	0.8520(2)	5.1(1)
C(3)	0.6075(2)	0.1232(2)	0.6173(2)	4.0(1)	C(20)	0.3937(2)	0.2293(2)	0.5869(2)	4.0(1)
C(4)	0.8145(2)	0.1286(2)	0.5477(2)	4.3(1)	C(21)	0.2934(2)	0.3404(2)	0.3766(2)	4.5(1)
C(5)	0.7827(2)	0.0610(2)	0.4072(2)	4.0(1)	C(22)	0.1929(2)	0.2671(2)	0.3118(2)	3.7(1)
C(6)	0.6984(2)	0.1006(2)	0.2830(2)	4.6(1)	C(23)	0.2234(2)	0.1722(2)	0.2362(2)	3.8(1)
C(7)	0.6710(2)	0.0368(3)	0.1544(3)	5.9(1)	C(24)	0.1301(2)	0.1066(2)	0.1716(2)	4.3(1)
C(8)	0.7318(3)	−0.0655(3)	0.1488(3)	6.7(2)	C(25)	0.0063(2)	0.1352(2)	0.1827(2)	4.8(1)
C(9)	0.8176(3)	−0.1049(2)	0.2684(4)	6.3(2)	C(26)	−0.0261(2)	0.2283(2)	0.2572(3)	5.1(1)
C(10)	0.8413(2)	−0.0424(2)	0.3972(3)	4.9(1)	C(27)	0.0671(2)	0.2935(2)	0.3220(3)	4.8(1)
C(11)	0.5745(2)	0.3464(2)	0.8782(2)	4.5(1)					
				[Ga(L3)]·2CH_3OH					
Ga(1)	0.24733(2)	0.50251(2)	0.57751(2)	2.637(9)	C(10)	0.3301(2)	0.3224(1)	0.5930(2)	3.36(9)
O(1)	0.1190(1)	0.5622(1)	0.5736(1)	3.36(6)	C(11)	0.4631(2)	0.4291(1)	0.6617(2)	3.32(9)
O(2)	−0.0406(2)	0.5385(1)	0.9036(1)	5.7(1)	C(12)	0.4319(2)	0.4369(1)	0.7573(1)	3.00(8)
O(3)	0.3129(1)	0.54819(9)	0.6971(1)	3.10(6)	C(13)	0.3560(2)	0.4967(1)	0.7689(1)	2.91(7)
O(4)	0.5010(2)	0.3418(1)	0.9914(1)	4.85(8)	C(14)	0.3266(2)	0.5029(2)	0.8574(2)	3.61(8)
O(5)	0.3156(1)	0.5804(1)	0.5082(1)	3.22(6)	C(15)	0.3740(2)	0.4527(2)	0.9329(2)	3.9(1)
O(6)	0.2357(2)	0.6744(1)	0.1306(1)	4.74(8)	C(16)	0.4499(2)	0.3947(1)	0.9215(2)	3.58(9)
O(7)	0.3029(2)	0.7224(1)	0.7364(1)	5.4(1)	C(17)	0.4782(2)	0.3866(1)	0.8332(2)	3.29(8)
O(8)	0.5130(2)	0.6388(2)	0.5680(1)	5.3(1)	C(18)	0.4680(3)	0.3432(2)	1.0801(2)	5.7(1)
N(1)	0.1833(1)	0.3925(1)	0.6341(1)	2.76(6)	C(19)	0.1654(2)	0.3450(1)	0.4700(2)	3.40(9)
N(2)	0.3724(1)	0.4098(1)	0.5853(1)	2.89(7)	C(20)	0.2421(2)	0.4475(1)	0.3708(1)	3.36(9)
N(3)	0.1831(1)	0.4368(1)	0.4486(1)	2.99(7)	C(21)	0.2540(2)	0.5396(1)	0.3453(1)	2.96(8)
C(1)	0.2123(2)	0.3240(1)	0.5725(1)	2.95(8)	C(22)	0.2866(2)	0.6008(1)	0.4157(1)	2.89(8)
C(2)	0.0714(2)	0.3999(1)	0.6377(2)	3.41(9)	C(23)	0.2942(2)	0.6852(1)	0.3874(2)	3.6(1)
C(3)	0.0541(2)	0.4793(1)	0.6908(2)	3.24(9)	C(24)	0.2769(2)	0.7077(1)	0.2928(2)	3.9(1)
C(4)	0.0788(2)	0.5585(1)	0.6534(2)	3.17(8)	C(25)	0.2494(2)	0.6465(1)	0.2237(2)	3.44(9)
C(5)	0.0584(2)	0.6322(1)	0.7012(2)	3.7(1)	C(26)	0.2366(2)	0.5627(1)	0.2500(2)	3.21(8)
C(6)	0.0174(2)	0.6286(2)	0.7839(2)	4.1(1)	C(27)	0.2330(3)	0.6121(2)	0.0601(2)	5.4(1)
C(7)	−0.0021(2)	0.5508(2)	0.8209(2)	4.0(1)	C(28)	0.2747(3)	0.7620(2)	0.6494(2)	5.8(1)
C(8)	0.0162(2)	0.4761(1)	0.7738(2)	3.8(1)	C(29)	0.5317(2)	0.6784(3)	0.6560(3)	7.3(2)
C(9)	−0.0691(3)	0.6100(2)	0.9509(2)	6.4(2)					

[a] $B_{eq} = (8/3)\pi^2\sum\sum U_{ij}a_i^*a_j^*(\mathbf{a}_i\mathbf{a}_j)$.

Table V. Bond Lengths (Å) in H_3L1' with Estimated Standard Deviations

O(1)–C(6)	1.367(3)	C(6)–C(7)	1.391(3)
O(2)–C(13)	1.380(3)	C(7)–C(8)	1.379(4)
O(3)–C(23)	1.370(2)	C(8)–C(9)	1.369(4)
N(1)–C(1)	1.486(2)	C(9)–C(10)	1.379(3)
N(1)–C(3)	1.465(2)	C(11)–C(12)	1.505(3)
N(1)–C(4)	1.473(2)	C(12)–C(13)	1.392(3)
N(2)–C(1)	1.486(2)	C(12)–C(17)	1.386(3)
N(2)–C(2)	1.486(2)	C(13)–C(14)	1.379(3)
N(2)–C(11)	1.483(2)	C(14)–C(15)	1.377(3)
N(3)–C(20)	1.469(3)	C(15)–C(16)	1.369(3)
N(3)–C(21)	1.469(3)	C(16)–C(17)	1.380(3)
C(1)–C(18)	1.518(3)	C(21)–C(22)	1.502(3)
C(1)–C(19)	1.532(3)	C(22)–C(23)	1.386(3)
C(2)–C(3)	1.517(3)	C(22)–C(27)	1.390(3)
C(2)–C(20)	1.515(3)	C(23)–C(24)	1.386(3)
C(4)–C(5)	1.507(3)	C(24)–C(25)	1.374(3)
C(5)–C(6)	1.390(3)	C(25)–C(26)	1.368(3)
C(5)–C(10)	1.386(3)	C(26)–C(27)	1.382(3)

Table VI. Bond Angles (deg) in H_3L1' with Estimated Standard Deviations

C(1)–N(1)–C(3)	104.9(1)	C(8)–C(9)–C(10)	119.5(3)
C(1)–N(1)–C(4)	116.3(1)	C(5)–C(10)–C(9)	121.5(3)
C(3)–N(1)–C(4)	113.1(2)	N(2)–C(11)–C(12)	110.8(2)
C(1)–N(2)–C(2)	108.0(2)	C(11)–C(12)–C(13)	119.8(2)
C(1)–N(2)–C(11)	115.5(2)	C(11)–C(12)–C(17)	122.2(2)
C(2)–N(2)–C(11)	113.0(2)	C(13)–C(12)–C(17)	117.9(2)
C(20)–N(3)–C(21)	112.2(2)	O(2)–C(13)–C(12)	120.3(2)
N(1)–C(1)–N(2)	99.7(2)	O(2)–C(13)–C(14)	118.7(2)
N(1)–C(1)–C(18)	109.8(2)	C(12)–C(13)–C(14)	121.0(2)
N(1)–C(1)–C(19)	113.3(2)	C(13)–C(14)–C(15)	119.4(2)
N(2)–C(1)–C(18)	110.0(2)	C(14)–C(15)–C(16)	120.9(2)
N(2)–C(1)–C(19)	113.4(2)	C(15)–C(16)–C(17)	119.3(2)
C(18)–C(1)–C(19)	110.1(2)	C(12)–C(17)–C(16)	121.5(2)
N(2)–C(2)–C(3)	104.4(2)	N(3)–C(20)–C(2)	112.1(2)
N(2)–C(2)–C(20)	111.8(2)	N(3)–C(21)–C(22)	111.5(2)
C(3)–C(2)–C(20)	112.7(2)	C(21)–C(22)–C(23)	120.5(2)
N(1)–C(3)–C(2)	103.8(2)	C(21)–C(22)–C(27)	121.4(2)
N(1)–C(4)–C(5)	111.5(2)	C(23)–C(22)–C(27)	118.1(2)
C(4)–C(5)–C(6)	121.9(2)	O(3)–C(23)–C(22)	121.4(2)
C(4)–C(5)–C(10)	120.0(2)	O(3)–C(23)–C(24)	118.1(2)
C(6)–C(5)–C(10)	118.1(2)	C(22)–C(23)–C(24)	120.5(2)
O(1)–C(6)–C(5)	121.5(2)	C(23)–C(24)–C(25)	120.0(2)
O(1)–C(6)–C(7)	117.7(2)	C(24)–C(25)–C(26)	120.6(2)
C(5)–C(6)–C(7)	120.8(2)	C(25)–C(26)–C(27)	119.3(2)
C(6)–C(7)–C(8)	119.3(2)	C(22)–C(27)–C(26)	121.5(2)
C(7)–C(8)–C(9)	120.8(2)		

Results and Discussion

Synthesis and Properties of Tap-based N_3O_3 Amine Phenols. Tap was prepared according to the reported method[10] with some modifications. The N_3O_3 Schiff bases were obtained from condensation reactions of tap with 3 equiv of salicylaldehyde or its ring-substituted derivatives. Reduction of the Schiff bases by KBH_4 in methanol produced the corresponding N_3O_3 amine phenols (Scheme I). H_3L1–H_3L3 are soluble in polar solvents such as chloroform and methanol while H_3L4 is only slightly soluble in DMSO. They are hydrolytically stable in solution under either basic or acidic conditions. All new N_3O_3 amine phenols (H_3L1–H_3L4) were characterized by a variety of spectroscopic methods (IR, NMR, and FAB-MS) and elemental analysis.

The IR spectra of the N_3O_3 Schiff bases contain very strong bands at 1620–1500 cm^{-1}, characteristic of imine C=N bond

Table VII. Bond Lengths (Å) in [Ga(L3)]·2CH_3OH with Estimated Standard Deviations

Ga(1)–O(1)	1.917(2)	C(1)–C(10)	1.519(3)
Ga(1)–O(3)	1.911(1)	C(1)–C(19)	1.522(3)
Ga(1)–O(5)	1.900(1)	C(2)–C(3)	1.500(3)
Ga(1)–N(1)	2.143(2)	C(3)–C(4)	1.413(3)
Ga(1)–N(2)	2.179(2)	C(3)–C(8)	1.373(3)
Ga(1)–N(3)	2.149(2)	C(4)–C(5)	1.394(3)
O(1)–C(4)	1.347(3)	C(5)–C(6)	1.391(4)
O(2)–C(7)	1.387(3)	C(6)–C(7)	1.373(3)
O(2)–C(9)	1.396(3)	C(7)–C(8)	1.395(3)
O(3)–C(13)	1.348(2)	C(11)–C(12)	1.507(3)
O(4)–C(16)	1.377(3)	C(12)–C(13)	1.399(3)
O(4)–C(18)	1.418(3)	C(12)–C(17)	1.390(3)
O(5)–C(22)	1.350(2)	C(13)–C(14)	1.396(3)
O(6)–C(25)	1.385(2)	C(14)–C(15)	1.389(3)
O(6)–C(27)	1.402(3)	C(15)–C(16)	1.381(3)
O(7)–C(28)	1.383(4)	C(16)–C(17)	1.390(3)
O(8)–C(29)	1.388(3)	C(20)–C(21)	1.505(3)
N(1)–C(1)	1.484(2)	C(21)–C(22)	1.402(3)
N(1)–C(2)	1.482(3)	C(21)–C(26)	1.392(3)
N(2)–C(10)	1.490(3)	C(22)–C(23)	1.392(3)
N(2)–C(11)	1.493(3)	C(23)–C(24)	1.381(3)
N(3)–C(19)	1.498(3)	C(24)–C(25)	1.379(3)
N(3)–C(20)	1.481(3)	C(25)–C(26)	1.386(3)

Table VIII. Bond Angles (deg) in [Ga(L3)]·2CH_3OH with Estimated Standard Deviations

O(1)–Ga(1)–O(3)	95.23(6)	O(1)–C(4)–C(3)	120.8(2)
O(2)–Ga(1)–O(5)	99.62(7)	O(1)–C(4)–C(5)	121.6(2)
O(1)–Ga(1)–N(1)	90.01(6)	C(3)–C(4)–C(5)	117.6(2)
O(1)–Ga(1)–N(2)	167.24(6)	C(4)–C(5)–C(6)	121.7(2)
O(1)–Ga(1)–N(3)	90.34(7)	C(5)–C(6)–C(7)	119.7(2)
O(3)–Ga(1)–O(5)	92.94(6)	O(2)–C(7)–C(6)	125.4(2)
O(3)–Ga(1)–N(1)	96.01(6)	O(2)–C(7)–C(8)	114.8(2)
O(3)–Ga(1)–N(2)	89.63(6)	C(6)–C(7)–C(8)	119.8(2)
O(3)–Ga(1)–N(3)	173.00(6)	C(3)–C(8)–C(7)	120.7(2)
O(5)–Ga(1)–N(1)	166.21(6)	N(2)–C(10)–C(1)	110.5(2)
O(5)–Ga(1)–N(2)	91.89(7)	N(2)–C(11)–C(12)	111.8(2)
O(5)–Ga(1)–N(3)	90.30(6)	C(11)–C(12)–C(13)	118.7(2)
N(1)–Ga(1)–N(2)	77.73(7)	C(11)–C(12)–C(17)	121.0(2)
N(1)–Ga(1)–N(3)	79.72(6)	C(13)–C(12)–C(17)	120.3(2)
N(2)–Ga(1)–N(3)	84.06(7)	O(3)–C(13)–C(12)	121.2(2)
Ga(1)–O(1)–C(4)	115.7(1)	O(3)–C(13)–C(14)	120.4(2)
C(7)–O(2)–C(9)	118.4(2)	C(12)–C(13)–C(14)	118.4(2)
Ga(1)–O(3)–C(13)	121.2(1)	C(13)–C(14)–C(15)	120.7(2)
C(16)–O(4)–C(18)	117.1(2)	C(14)–C(15)–C(16)	120.6(2)
Ga(1)–O(5)–C(22)	126.3(1)	O(4)–C(16)–C(15)	125.2(2)
C(25)–O(6)–C(27)	117.2(2)	O(4)–C(16)–C(17)	115.7(2)
Ga(1)–N(1)–C(1)	101.3(1)	C(15)–C(16)–C(17)	119.1(2)
Ga(1)–N(1)–C(2)	114.2(1)	C(12)–C(17)–C(16)	120.7(2)
C(1)–N(1)–C(2)	116.2(2)	N(3)–C(19)–C(1)	110.9(2)
Ga(1)–N(2)–C(10)	109.3(1)	N(3)–C(20)–C(21)	112.6(2)
Ga(1)–N(2)–C(11)	113.1(1)	C(20)–C(21)–C(22)	120.8(2)
C(10)–N(2)–C(11)	112.9(2)	C(20)–C(21)–C(26)	118.9(2)
Ga(1)–N(3)–C(19)	109.6(1)	C(22)–C(21)–C(26)	120.2(2)
Ga(1)–N(3)–C(20)	114.8(1)	O(5)–C(22)–C(21)	122.7(2)
C(19)–N(3)–C(20)	112.7(2)	O(5)–C(22)–C(23)	119.3(2)
N(1)–C(1)–C(10)	105.1(2)	C(21)–C(22)–C(23)	117.9(2)
N(1)–C(1)–C(19)	108.4(2)	C(22)–C(23)–C(24)	121.5(4)
C(10)–C(1)–C(19)	114.0(2)	C(23)–C(24)–C(25)	120.2(2)
N(1)–C(2)–C(3)	109.0(2)	O(6)–C(25)–C(24)	116.4(2)
C(2)–C(3)–C(4)	118.0(2)	O(6)–C(25)–C(26)	124.1(2)
C(2)–C(3)–C(8)	121.5(2)	C(24)–C(25)–C(26)	119.5(2)
C(4)–C(3)–C(8)	120.4(2)	C(21)–C(26)–C(25)	120.5(2)

stretches. The ^1H NMR spectra display the resonance signals at ~8.3 ppm due to imine hydrogens (Table IX). Upon reduction, the characteristic imine C=N stretches disappear and two new bands appear at 1610–1580 cm^{-1}, probably from N–H bending modes. The ^1H NMR spectra of amine phenols (Table X) show the presence of benzylic signals at ~4 ppm instead of the CH=N imine hydrogen signals at ~8.3 ppm. These observations confirm that the C=N bonds have been reduced to the CH_2—NH linkages.

The reaction of H_3L1 with acetone produces a new N_3O_3 amine phenol H_3L' (Scheme II) which contains a five-membered imidazolidine ring. Under similar conditions the tren- and tame-based amine phenol ligands do not form the acetone adduct,

Scheme I

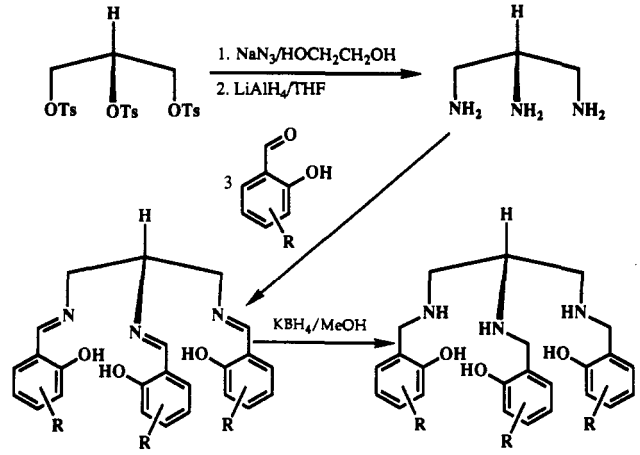

Table IX. ^1H NMR (200 MHz) Data for Schiff Bases (δ in ppm from TMS; $CDCl_3$)

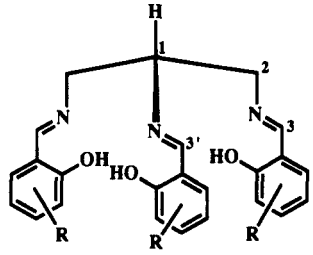

	H_3saltap	H_3Cl-saltap	H_3psaltap	H_3Cl_2saltap
H(1)	3.90 (m, 1H)	3.90 (m, 1H)	3.90 (m, 1H)	3.90 (m, 1H)
H(2)	3.95 (q, 4H)	3.95 (q, 4H)	3.95 (q, 4H)	4.00 (q, 4H)
H(3)/H(3′)	8.30 (s, 3H)	8.30 (s, 3H)	8.30 (s, 3H)	8.30 (s, 3H)
OCH_3			3.70 (s, 3H)	
			3.75 (s, 6H)	
OH	12.7 (b s, 1H)	12.0 (b s, 1H)	12.5 (b s, 1H)	13.5 (b s, 1H)
	13.4 b s, 2H)	13.0 (b s, 2H)	12.8 (b s, 2H)	13.7 (b s, 2H)
aromatic H	6.90 (m, 6H)	6.90 (m, 3H)	6.70 (m, 3H)	7.15 (d, 3H)[a]
	7.20 (m, 6H)	7.20 (m, 6H)	6.86 (m, 6H)	7.40 (d, 3H)[a]

[a] $^3J_{H-H}$ = 7.0–8.0 Hz; $^4J_{H-H}$ = 2.0–2.5 Hz.

Table X. ^1H NMR (200 MHz) Data for N_3O_3 Amine Phenols (δ in ppm from TMS; $CDCl_3$)

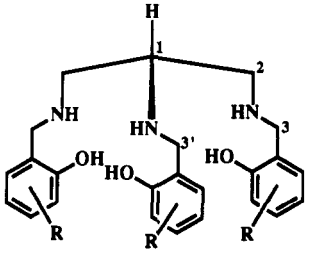

	H_3L1	H_3L2	H_3L3	H_3L4[a]
H(1)	2.85 (m, 1H)	2.85 (m, 1H)	2.75 (m, 1H)	2.90 (m, 1H)
H(2)	2.75 (d, 4H)	2.75 (d, 4H)	2.65 (b s, 4H)	2.70 (d, 4H)
H(3)	3.95 (q, 4H)	3.85 (q, 4H)	3.70 (q, 4H)	3.90 (b s, 4H)
H(3′)	3.85 (s, 2H)	3.75 (s, 2H)	3.80 (s, 2H)	3.70 (s, 2H)
OCH_3			3.65 (s, 9H)	
O–H/N–H	6.00 (b s)	6.00 (b s)	6.00 (b s)	7.00 (b s)
aromatic H	6.70–7.30 (m, 12H)	6.50–7.30 (m, 9H)	6.40–6.80 (m, 9H)	6.80–7.50 (m, 6H)

[a] In DMSO-d_6.

probably because of the lack of hydrogen atoms on the tertiary N and the instability of the six-membered ring which would form, respectively. H_3L' was characterized by spectroscopic methods (IR, NMR, and FAB-MS), elemental analysis, and X-ray crystallography.

Crystal Structure of H_3L'. An ORTEP drawing of H_3L' is illustrated in Figure 1. Bond lengths and bond angles are listed

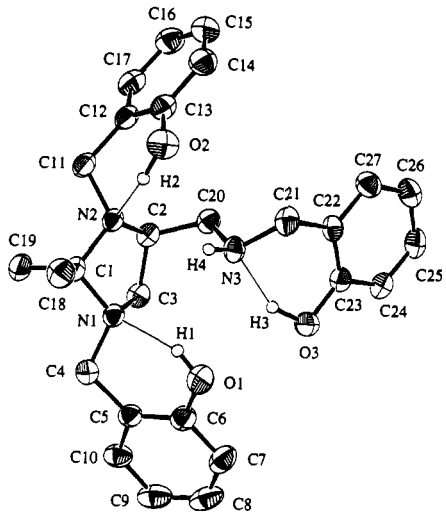

Figure 1. ORTEP drawing of H_3L' ($C_{27}H_{33}N_3O_3$). 33% probability thermal ellipsoids are shown for the non-hydrogen atoms; fine lines represent hydrogen bonds.

Scheme II

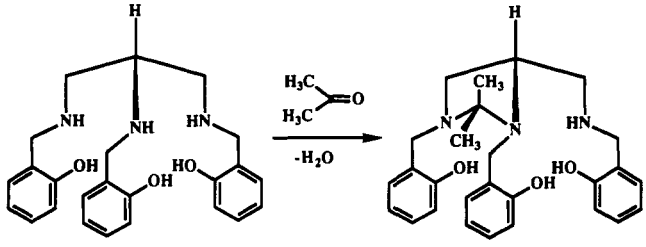

in Tables V and VI, respectively. There are two H_3L' molecules in each triclinic unit cell. Each molecule is highly preorganized with all six heteroatoms (N_3O_3) being correctly oriented for metal complexation. The high degree of preorganization is aided by the formation of a five-membered imidazolidine ring but is primarily dictated by the presence of three strong intrastrand H-bonds (O(1)–H(1)- - -N(1) = 1.99(2) Å, O(2)–H(2)- - -N(2) = 1.99(3) Å, and O(3)–H(3)- - -N(3) = 1.70(3) Å) and a very weak interstrand H-bond (N(3)–H(4)- - -N(2) = 2.48(2) Å). The observation of the interstrand H-bond is significant. This suggests that the tren-based N_4O_3 and tame/tap-based N_3O_3 tripodal amine phenols might also be significantly preorganized by forming intrastrand and interstrand H-bonds. The five-membered imidazolidine ring H_3L' adopts an envelope conformation with C(1) lying 0.59 Å out of the plane defined by N(1), C(3), C(2), and N(2). The two methyl groups on C(1) are nonequivalent, as evinced by the ^1H NMR spectrum of H_3L' (Figure 2). The N(1)–C(3)–C(2)–N(2) and N(2)–C(2)–C(20)–N(3) units in H_3L' adopt *gauche* conformations (torsion angles: N(1)–C(3)–C(2)–N(2) = –16.2°; N(2)–C(2)–C(20)–N(3) = 58.1°) because of the five-membered imidazolidine ring formation and the hydrogen bonding between H(4) and N(2) atoms, respectively.

Each strand in a tripodal amine phenol molecule contains two functional groups: a secondary amine NH and a phenolic OH. Since the most acidic proton is the phenolic proton ($pK \sim 7.0$),[13] it is not unexpected that the intrastrand H-bonds are formed between phenolic hydrogens and amine nitrogens rather than those between amine hydrogens and phenolic oxygens. There are two possible interstrand H-bonds: N(3)–H(4)- - -N(2) and N(3)–H(4)- - -O(2). The N(2)- - -H(4) distance of 2.48(2) Å (with N(3)- - -N(2) = 2.937(2) Å and N(3)–H(4)- - -N(2) = 111(1)°) shows that the interstrand H-bond is very weak. The O(2)- - -H(4) distance is 2.78(2) Å, too long to be considered a H-bond. The weak N(2)- - -H(4) H-bond and a long O(2)- - -H(4) distance are probably caused by the rigidity of the five-membered imidazolidine ring, which stiffens portions of the molecule and keeps two arms far away from the third one. From this point of view, interstrand N–H- - -N and N–H- - -O H-bonds should be stronger in the tripodal amine phenols than they are in H_3L'.

Polydentate ligands with three-dimensional cavities are of particular interest because of the high stability of their complexes, the substantial selectivity in their binding by enforcing a specific spatial arrangement of donor atoms or by introducing different donor atoms, and their capability to adopt a preorganized conformation in the uncomplexed state. The preorganization of a tripodal ligand can be achieved by introducing a rigid tripodal framework[14–16] and/or by forming intrastrand and interstrand H-bonds.[17–22] The intra- and interstrand H-bonds will generate a propeller-like structure in which all donor atoms are correctly oriented for metal ion complexation (shown schematically in diagram A). In our previous contributions,[5–8] we reported several

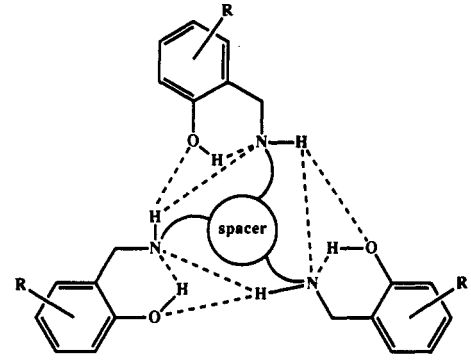

A

N_4O_3 and N_3O_3 tripodal amine phenol ligands but were unsuccessful in crystallizing an uncomplexed amine phenol. Although intrastrand and interstrand H-bonds were found in the coordinated amine phenol ligands in $[Ln(H_3L)_2]^{3+}$ (Ln = Pr, and Gd; H_3L = tris(((2-hydroxy-3-methoxybenzyl)amino)ethyl)amine),[18] we had no evidence for the intrastrand and interstrand H-bond formation in the solid state in free amine phenols. The structural study of H_3L' has for the first time, in this work, revealed evidence of strong intrastrand (O–H- - -N) and weak interstrand (N–H- - -N) H-bonds, which, at least in part, may contribute to the preorganized frameworks of all these tripodal amine phenols.

^1H NMR Spectra of H_3L'. The 500-MHz ^1H NMR spectrum is illustrated in Figure 2. The spectral assignments are tentative and were made on the basis of ^1H–^1H COSY, APT (attached proton test), and ^1H–^{13}C heteronuclear correlation spectra. The two hydrogens or carbons on a single carbon atom were distinguished by the fact that hydrogens in pseudoaxial environments are more shielded than those in pseudoequatorial environments.[23]

(13) Garrett, T. M.; Miller, P. W.; Raymond, K. N. *Inorg. Chem.* **1989**, *28*, 128.

(14) Cram, D. J. *Angew. Chem., Int. Ed. Engl.* **1988**, *27*, 1021.
(15) Lehn, J.-M. *Angew. Chem., Int. Ed. Engl.* **1988**, *27*, 89.
(16) Seel, C.; Vögtle, F. *Angew. Chem., Int. Ed. Engl.* **1992**, *31*, 528.
(17) Karpishin, T. B.; Stack, T. D. P.; Raymond, K. N. *J. Am. Chem. Soc.* **1993**, *115*, 182.
(18) Garrett, T. M.; Cass, M. E.; Raymond, K. N. *J. Coord. Chem.* **1992**, *25*, 241.
(19) Tor, Y.; Libman, J.; Shanzer, A.; Felder, C. E.; Lifson, S. *J. Am. Chem. Soc.* **1992**, *114*, 6653.
(20) Tor, Y.; Libman, J.; Shanzer, A.; Felder, C. E.; Lifson, S. *J. Am. Chem. Soc.* **1992**, *114*, 6661.
(21) Shanzer, A.; Libman, J.; Lifson, S. *Pure Appl. Chem.* **1992**, *64*, 1421.
(22) Libman, J.; Tor, Y.; Dayan, I.; Shanzer, A.; Lifson, S. *Isr. J. Chem.* **1992**, *32*, 31.
(23) Silverstein, R. M.; Bassler, G. C.; Morrill, T. C. *Spectrometric Identification of Organic Compounds*, 4th ed.; John Wiley & Sons: New York, 1981; p 189.

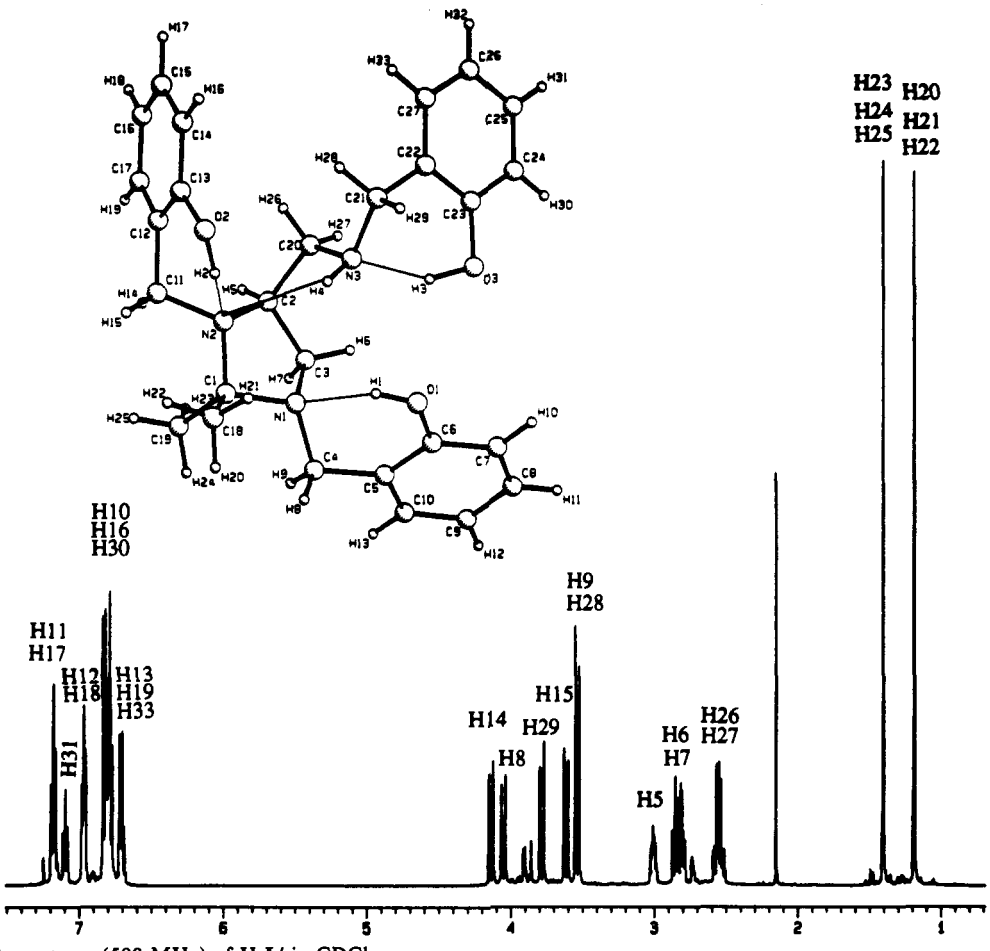

Figure 2. ^1H NMR spectrum (500-MHz) of H_3L' in $CDCl_3$.

In H_3L' all three chelating arms are different because of the asymmetric nature of the molecule. Consequently, three overlapped AB quartets from three pairs of benzylic hydrogens are seen at 3.4–4.3 ppm in the ^1H NMR spectrum. The inequivalency of two benzylic hydrogens on C(4) (or C(11)) and C(21) are probably caused by the chirality of the N atoms of the imidazolidine ring and by the long-range effect of the chirality of C(2), respectively. The ^1H NMR spectrum of H_3L' in DMSO-d_6 is very similar to that in $CDCl_3$ while in CD_3OD decomposition was observed. Due to the high polarity of DMSO and methanol, intra- and interstrand H-bonds are expected to be weakened.[18] Variable-temperature (21–50 °C) ^1H NMR spectra of H_3L' in $CDCl_3$ showed no significant changes in the spectra. These observations suggest that the H_3L' molecule remains relatively rigid in solution and the rigidity arises from five-membered imidazolidine ring formation rather than intra- and interstrand hydrogen bonding.

Metal Complexes. Neutral complexes [M(L)] (M = Ga, In; L = **L1**–**L4**) were easily prepared from reactions of amine phenols (H_3**L1**–H_3**L4**) with hydrated metal nitrates or perchlorates in the presence of a base (hydroxide or acetate). H_3L' forms [M(**L1**)] complexes with group 13 metal ions; the five-membered imidazolidine ring is opened upon coordination to the metal ion. Preparation of the aluminum complexes [Al(L)] (L = **L1**–**L4**) was often accompanied by the precipitation of aluminum hydroxide, especially in the presence of excess sodium hydroxide. Attempts to isolate pure aluminum complexes [Al(L)] (L = **L1**, **L3**) were unsuccessful because of contamination by aluminum hydroxide. The gallium and indium complexes were all stable under both basic (no metal hydroxide forms in presence of sodium hydroxide) and weakly acidic conditions (acetic acid is formed when the metal ion reacts with an N_3O_3 amine phenols in the presence of 3–4 equiv of sodium acetate). The metal complexes isolated were soluble in DMSO and slightly soluble in methanol or acetone. All of them were characterized by IR, NMR (^1H and ^{13}C), and FAB mass spectroscopic methods, as well as by elemental analysis and in the case of [Ga(**L3**)]·$2CH_3OH$ by X-ray crystallography.

All complexes show IR bands at 3270–3250 cm^{-1} due to N–H stretches of the coordinated secondary amine groups and at 1595–1560 cm^{-1} due to N–H bending vibrations (Table II). Upon coordination to the metal ion, the N–H bending frequencies undergo a general bathochromic shift (about 20 cm^{-1}). The observation of broad bands at 3650–3000 cm^{-1} from O–H stretches suggests the presence of hydrogen bonding in most complexes. New bands appear below 600 cm^{-1} in the spectrum of each coordinated ligand, and they are most likely ν(M–O) or ν(M–N); however, assignments of these bands are not definitive because of the low energies associated with these vibrations.

The FAB mass spectra of all complexes were obtained in a 3-nitrobenzyl alcohol matrix in the positive-ion detection mode (Table II). In general, for all complexes the molecular ion peaks were detected, and in the spectra of many of the complexes, dimeric peaks were also detected.

X-ray Crystal Structure of [Ga(L3)]·2CH_3OH. An ORTEP drawing of [Ga(**L3**)]·$2CH_3OH$ is illustrated in Figure 3. Bond lengths and angles are listed in Tables VII and VIII, respectively. In the monoclinic unit cell there are four [Ga(**L3**)] molecules (two pairs of Λ and Δ enantiomers), each with two associated molecules of methanol. One methanol in [Ga(**L3**)]·$2CH_3OH$ is hydrogen-bonded to a phenolate oxygen (O(3)- - -H(1) = 1.87(4) Å), while the other methanol is hydrogen-bonded to phenolate O(5) (O(5)- - -H(2) = 1.94(3) Å) and an amine hydrogen (O(8)- - -H(4) = 2.10 Å) of the nearest [Ga(**L3**)·$2CH_3OH$ neighbor.

(24) Rauk, A.; Allen, L. C.; Mislow, K. *Angew. Chem., Int. Ed. Engl.* **1970**, *9*, 400.

Table XI. ^{1}H NMR Data for Metal Complexes of Tap-Based Amine Phenols (200 MHz; in DMSO-d_6)[a]

complex	aromatic hydrogens	benzylic hydrogens, methylene hydrogens, and hydrogens on coordinated N atoms
[Al(**L2**)]	7.00 (m, 5H), 6.85 (m, 1H), 6.65 (d, 1H), 6.40 (d, 1H), 5.82 (d, 1H)	4.90 (m, 1H), 4.70 (t, 1H), 4.25 (t, 1H), 4.05 (d, 1H), 3.70 (t, 1H), 3.60–3.30 (m, 5H), 3.20 (m, 1H), 3.02 (t, 1H), 2.80 (b s, 1H), 2.38 (t, 1H)
[Al(**L4**)]	7.38 (d, 1H), 7.14 (d, 1H), 7.12 (d, 1H), 7.06 (d, 1H), 7.02 (d, 1H), 6.85 (d, 1H)	5.10 (b s, 1H), 4.86 (t, 1H), 4.28 (t, 1H), 4.05 (d, 1H), 3.68 (t, 1H), 3.56 (d, 1H), 3.48 (m, 2H), 3.38 (m, 1H), 3.25 (m, 1H), 3.05 (m, 1H), 2.80 (b s, 1H), 2.55 (m, 1H), 2.35 (t, 1H)
[Ga(**L1**)]	7.00 (m, 3H), 6.90 (m, 3H), 6.70 (d, 1H), 6.55 (d, 1H), 6.40 (m, 3H), 5.64 (d, 1H)	4.80–4.60 (m, 2H), 4.40–4.00 (m, 3H), 3.80 (t, 1H), 3.50 (m, 2H), 3.30–3.10 (m, 2H), 2.80 (b s, 1H), 2.70 (m, 1H), 2.60 (m, 1H), 2.30 (t, 1H)
[Ga(**L2**)]	7.10–6.90 (m, 4H), 6.80 (m, 2H), 6.70 (d, 1H), 6.50 (d, 1H), 5.70 (d, 1H)	4.90 (m, 2H), 4.30 (t, 1H), 4.10 (d, 1H), 3.70 (t, 1H), 3.50 (d, 1H), 3.60–3.30 (m, 5H), 2.80 (b s, 1H), 2.60 (m, 1H), 2.38 (t, 1H)
[Ga(**L3**)]	6.80–6.50 (m, 5H), 6.50–6.30 (m, 3H), 5.60 (d, 1H)	4.70 (b s, 1H), 4.50 (b s, 1H), 4.40–4.00 (m, 3H), 3.80 (d, 1H), 3.70–3.40 (m, 3H), 3.65 (s, 3H), 3.60 (s, 3H), 3.55 (s, 3H), 3.20 (m, 2H), 2.80 (b s, 1H), 2.84 (m, 1H), 2.50 (t, 1H)
[Ga(**L4**)]	7.30 (d, 1H), 7.15 (d, 1H), 7.12 (d, 1H), 7.06 (d, 1H), 7.00 (d, 1H), 6.85 (d, 1H)	5.05 (m, 2H), 4.38 (t, 1H), 4.15 (d, 1H), 3.75 (t, 1H), 3.65 (m, 2H), 3.45 (m, 2H), 3.30 (m, 1H), 3.15 (m, 1H), 2.85 (b s, 1H), 2.65 (m, 1H), 2.30 (t, 1H)
[In(**L1**)]	7.00 (m, 3H), 6.85 (m, 3H), 6.65 (m, 2H), 6.40 (m, 3H), 6.16 (d, 1H)	4.90 (b s, 1H), 4.70 (t, 1H), 4.40 (t, 1H), 3.95 (m, 2H), 3.70 (d. 1H), 3.50 (m, 3H), 3.30 (m, 2H), 2.90 (b s, 1H), 2.8–2.50 (m, 2H)
[In(**L2**)]	7.10–6.80 (m, 6H), 6.65 (d, 1H), 6.58 (d, 1H), 6.18 (d, 1H)	5.04 (b s, 1H), 4.85 (t, 1H), 4.38 (t, 1H), 4.10 (b s, 1H), 4.00 (d, 1H), 3.90 (m, 2H), 3.55 (m, 3H), 3.28 (t, 1H), 2.90 (b s, 1H), 2.68 (m, 1H), 2.50 (t, 1H)
[In(**L3**)]	6.80–6.40 (m, 8H), 6.05 (d, 1H)	4.85 (b s, 1H), 4.60 (b s, 1H), 4.40 (t, 1H), 3.95 (m, 2H), 3.80–3.35 (m, 5H), 3.65 (s, 3H), 3.60 (s, 3H), 3.57 (s, 3H), 3.20 (d, 1H), 2.85 (b s, 1H), 2.65 (m, 1H), 2.50 (m, 1H)
[In(**L4**)]	7.30 (d, 1H), 7.20 (d, 1H), 7.16 (d, 1H), 7.10 (d, 1H), 7.00 (d, 1H), 6.88 (d, 1H)	5.15 (m, 1H), 5.00 (b s, 1H), 4.45 (t, 1H), 4.30–3.35 (m, 5H), 3.25 (m, 2H), 3.15 (m, 1H), 2.85 (b s, 1H), 2.70 (m, 1H), 2.40 (t, 1H)

[a] $^3J_{H-H}$(methylene hydrogens) = 12.5–15.0 Hz, $^3J_{H-H}$(aromatic hydrogens) = 6.5–8.0 Hz; $^4J_{H-H}$ = 2.0–2.5 Hz.

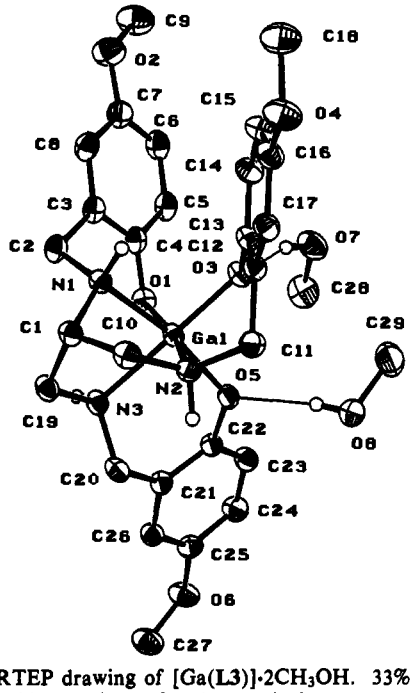

Figure 3. ORTEP drawing of [Ga(**L3**)]·2CH_3OH. 33% probability thermal ellipsoids are shown for the non-hydrogen atoms; fine lines represent hydrogen bonds.

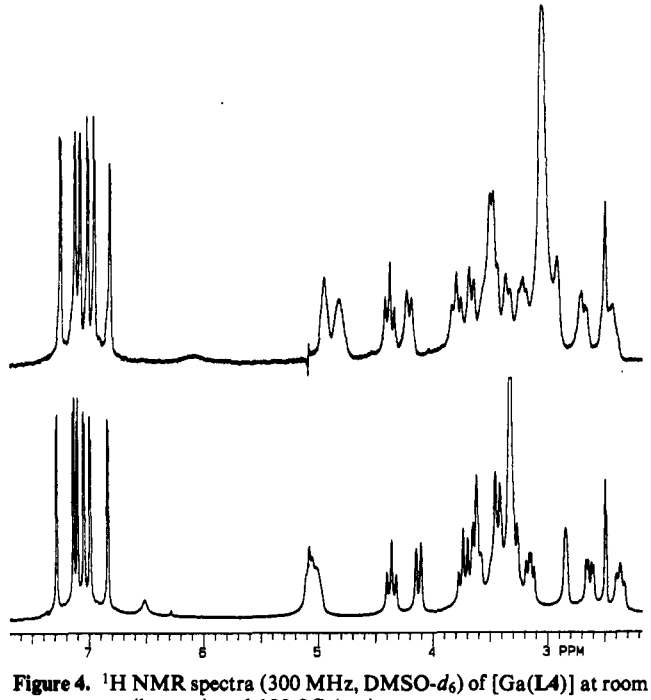

Figure 4. ^{1}H NMR spectra (300 MHz, DMSO-d_6) of [Ga(**L4**)] at room temperature (bottom) and 120 °C (top).

The complex is neutral with a triply deprotonated N_3O_3 amine phenol ligand completely encapsulating the Ga^{3+} ion. Each N_3 and O_3 donor set coordinates to the Ga^{3+} ion in a facial manner to form a distorted octahedral coordination geometry. The distortion of the coordination sphere is most evident in the compression of the N–Ga–N angles (which average 80.5°) and in the expansion of the O–Ga–O angles (which average 95.9°). As a result, the three trans N–Ga–O angles deviate from 180° (O(1)–Ga(1)–N(2) = 167.24(6)°, O(3)–Ga(1)–N(3) = 173.00(6)°, and O(5)–Ga(1)–N(1) = 166.21(6)°). Apparently the degree of distortion in [Ga(**L3**)]·2CH_3OH is larger than that in its tame-based analog (Chart I) with an extra methylene unit in [Ga(**IIa**)]·H_2O (average N–Ga–N = 85.5° and O–Ga–O = 93.2°)[7] because of the shortening of one of the three chelating arms. The average Ga–O distance is 1.91 Å while the Ga–N bond lengths average to 2.16 Å. These values compare well with those in [Ga(**IIa**)]·H_2O (average Ga–N = 2.13 Å and Ga–O = 1.92 Å)[7] and those in [Ga(**IIc**)]$^+$ (average Ga–N = 2.11 Å and Ga–O = 1.90 Å).[6]

Metal Complex NMR. The ^{1}H NMR spectra of the complexes in DMSO-d_6 (Table XI) are all very similar except for those resonance signals from the aromatic hydrogens in the region 6.4–7.5 ppm; only that (Figure 4) of [Ga(**L4**)] is discussed as a representative example. Due to the complexity of these spectra, detailed assignments were not made.

In the metal complexes, all three arms are different as a result of the asymmetric binding of the ligand to the metal center.

Therefore, every hydrogen (the six benzylic hydrogens on C(2), C(11), and C(20), the five methylene hydrogens on C(1), C(10), and C(19), and the three hydrogens on the coordinated N atoms N(1), N(2), and N(3); numbering from Figure 3) is in a magnetically distinct environment. Several overlapped multiplets were observed in the 2.0–5.6 ppm aliphatic region of the spectrum, and these remain as multiplets at temperatures up to 120 °C (Figure 4). The inequivalence of the three chelating arms was also evinced by the presence of three singlets from each of the three distinctive methoxy groups in the spectra of the [M(**L3**)] complexes. These observations clearly demonstrate the rigid structure of these complexes in solution and are consistent with the solid-state structure of [Ga(**L3**)]. This conclusion is also supported by the ^{13}C spectrum of [Ga(**L2**)], which shows 24 distinct resonances from the 24 different carbon atoms of the coordinated amine phenol ligand. If the complex were fluxional, only 18 carbon resonance signals would be expected, as was observed in the spectrum of the uncomplexed amine phenol.

Since all the complexes have similar structures, variable-temperature (21–120 °C) ^1H NMR spectra were obtained for only some representatives [M(L)] (M = Ga, In, L = **L3**; M = Al, Ga, In, L = **L4**) in order to examine their fluxional behavior in DMSO. There are no significant changes in the spectral parameters except for some minor shifts of the hydrogen signals in the aliphatic region (Figure 4). These shifts are probably caused by the thermal vibrations of the coordinated ligand framework. These observations clearly show that the aluminum, gallium, and indium complexes remain very rigid in DMSO solution.

Concluding Remarks. A new series of N_3O_3 amine phenols were readily prepared by the KBH_4 reduction of Schiff bases derived from reactions of tap with salicylaldehyde or its ring-substituted derivatives. Reaction of H_3**L1** with acetone produces a new amine phenol (H_3L') which was crystallographically characterized and shown to have all the heteroatoms correctly oriented for metal complexation. The preorganization of a tripodal amine phenol ligand can be achieved by forming intra- and interstrand H-bonds, as evinced by the structural data of H_3L'.

Like that of the tame-based N_3O_3 analogs,[7] the cavity of the tap-based N_3O_3 amine phenol ligand seems to be very flexible through the three chelating arms. However, shortening of one of the three chelating arms changes the symmetry of, and the binding in, their metal complexes. In [Ga(**II**)]·H_2O,[7] all chelate rings are six-membered (N–C–C–C–N–M) and the complex has a C_3 axis through the C bridgehead and the metal atom. In [Ga(**L3**)]·$2CH_3OH$, however, there is only one six-membered (N–C–C–C–N–M) and two five-membered (N–C–C–N–M) chelate rings and all the three chelating arms bind to the metal in different fashions.

The complex stability is closely related to the size of the chelate rings and the size of the bonded metal ion.[25-27] Generally, the complex stability decreases as the size of the chelate ring increases from five to six. The complexes of large metal ions are destabilized more than those of small metal ions by an increase in chelate ring size from five to six. Molecular mechanics calculations have revealed that smaller metal ions with M–N bond lengths close to 1.6 Å coordinate with the least steric strain to six-membered chelate rings while larger metal ions coordinate with the least steric strain to five-membered chelate rings of the en (ethylenediamine) type.[25-27] On the basis of structural data, the size of the cavity of the tame-based amine phenol ligand (all chelate rings are six-membered) matches best the size of Al^{3+} while the size of the cavity of the tap-base amine phenol ligand (there are two five-membered chelate rings and only one six-membered ring) is expected to match the size of Ga^{3+} best. Stability constant studies will better quantify this fit, and these are in progress.

Acknowledgment is made to the Natural Sciences and Engineering Research Council of Canada for an NSERC Postdoctoral Fellowship (S.L.) and an operating grant (C.O.) and to the U.S. Public Health Service for an operating grant (CA 48964). We also thank Professor J. Trotter for the very kind use of his crystallographic facilities.

Supplementary Material Available: Complete tables of crystallographic data, hydrogen atom parameters, anisotropic thermal parameters, intramolecular distances and angles involving hydrogen atoms, torsion angles, intermolecular contacts, and least-squares planes for each of the two structures (33 pages). Ordering information is given on any current masthead page.

(25) Hancock, R. D. *Prog. Inorg. Chem.* **1989**, *37*, 187.
(26) Hancock, R. D.; Martell, A. E. *Chem. Rev.* **1989**, *89*, 1875.
(27) Hancock, R. D. *J. Chem. Educ.* **1992**, *69*, 615.